

2D Optical-Thermal-Electrical Simulation for high Wall Plug Efficiency Cubic GaN green LED on Silicon

Jaekwon Lee^{1,2}

¹Department of Electrical and Computer Engineering, University of Illinois at Urbana-Champaign, Illinois, 61801, USA

²Micro and Nanotechnology Laboratory, University of Illinois at Urbana-Champaign, Illinois, 61801, USA

Abstract

Despite the relative success of the phosphor-converted Solid State Lighting (SSL), the need for high-efficiency green LED, especially at high current densities, has been emphasized over the past two decades. Cubic InGaN-based LEDs on Silicon are a promising platform to realize high-efficiency green emission. Their superior properties over their hexagonal counterparts are apparent in the literature, with no doubt dictating higher Internal Quantum Efficiency (IQE) than the conventional InGaN-based green LEDs. However, there are almost no studies on the cubic GaN LED itself, and especially there are no studies on their aspects other than the IQE: light extraction, junction temperature, peak emission wavelength, etc. These properties can actually be pointed out as weaknesses of cubic GaN LEDs compared to hexagonal ones, which deems this study critical for the realization of high Wall Plug Efficiency(WPE) green LED. Here, the 2D optical-thermal-electrical modeling of cubic GaN green LED on Silicon is suggested, and several designs are simulated to solve the issue of light extraction, junction temperature, and peak emission wavelength, which are mostly limited by the current crowding. As a result, it is found that DOE 2025 Goal for green LEDs can be achieved theoretically by the flip-chip vertical LED design.

I. Introduction

Since the high-brightness candela-class blue InGaN LED has been invented in 1994¹, GaN-based Solid State Lighting has achieved great success by producing white light with the blue light from the LEDs and yellow light from Phosphor conversion. However, due to the significant loss in phosphors and their theoretical limit, it is predicted that the luminous efficacy of those Phosphor-Converted LEDs (PC-LED) will saturate at 250 lm/W. Contrary to these PC-LEDs, the true white color can be achieved by mixing red, green, and blue light, achieving an ultimate upper potential of 330 lm/W. The necessity of this ultimate SSL utilizing Color-Mixed LEDs (CM-LED) has been emphasized by the federal government and local municipalities, including the Department of Energy (DOE)². This will enable a new and accelerated SSL roadmap, as early adoption of the ultimate SSL will induce significant energy savings and environmental benefits. In this path, although high WPE red and blue LEDs are developed with high reliability and are well commercialized, the need for high WPE green LED is urgent and yet remains unsolved. This is the issue that prevents this CM-LED approach, and it is called the “green gap³.” It is observed that GaN-based or GaP-based LEDs have significantly lower performance in the green wavelength. Especially, GaN-based green LEDs suffer from high defect density due to higher indium content than blue LEDs, low IQE and high efficiency droop due to the existence of polarization, and significant blueshift of the spectrum due to Quantum Confined Stark Effect (QCSE). These are the representative issues, and there are more issues than it appears, mostly due to the existence of polarization. For instance, polarization strongly hinders the hole transport in green Multi Quantum Well (MQW) LED, leading to the uneven carrier distribution among Quantum Wells at high bias and preventing MQW solution from solving the efficiency droop issue.⁴

Instead of conventional GaN LEDs using GaN as a Wurtzite (hexagonal) phase, green LEDs using Zincblende (cubic) GaN have appeared as a promising solution. Cubic GaN has favorable properties compared to hexagonal GaN in the LED field. First of all, it does not have polarization in the <100> growth direction thanks to its centrosymmetry. It is widely accepted that the absence of polarization will

increase the IQE of the LED. Also, it is expected to have smaller Auger Coefficients⁵ and larger Radiative recombination Coefficient⁶ than hexagonal GaN due to its band structure and smaller heavy-hole effective mass⁷. Finally, it is demonstrated that it has lower Mg doping activation energy and higher hole mobility⁸, assuring higher maximum achievable doping density for better ohmic contact. Due to its superior properties, cubic GaN is already popularly researched for green LEDs, and even commercial LEDs are researched.⁹ As cubic GaN is a metastable phase, it is extremely challenging to synthesize pure cubic GaN using commercial Metal Organic Chemical Vapor Deposition (MOCVD), and people usually achieved this by the direct deposition of GaN on cubic substrates such as 3C-SiC and GaAs. Especially, 3C-SiC is used as a common substrate for direct deposition as it shows low lattice mismatch (~3.5%) with cubic GaN in (100) direction¹⁰. Unfortunately, it often results in highly defective film and gives rise to the mixed-phase of hexagonal and cubic GaN as a form of hexagonal inclusion¹¹. Instead of direct deposition, a promising approach is to deposit GaN on the (111) plane of the nanopatterned Silicon (100)¹². In this method, the hexagonal GaN undergoes phase transition so that pure cubic GaN can be grown atop. It is very promising as they are low-defect, CMOS compatible, and single-phase. The research to achieve thin-film cubic GaN from this method is passionately researched. Due to the abovementioned reasons, cubic GaN on Silicon (100) will become a popular way to create a cubic GaN LED device.

In this regard, this project will be based on green-wavelength InGaN-based LED grown on Silicon (100). There are not so many papers that simulate the cubic InGaN-based LED, but it is widely known that cubic LEDs theoretically have much higher performance than its hexagonal counterpart¹³. Especially, one of the properties I want to briefly mention is that we can grow thicker Quantum Well without compromising the performance thanks to the absence of polarization. Therefore, thick Quantum Well design is a high-efficiency design for cubic GaN LED, which has higher IQE and longer emission wavelength. However, currently there are no studies, to my knowledge, that deal with other aspects of cubic GaN LED: junction temperature, Light Extraction Efficiency (LEE), or the emission from higher levels due to wider quantum well width. Especially, the ultimate goal of the LED is not the high IQE: according to the DOE report, the 2025 goal for the green LED is to achieve >30% WPE at 100A/cm² current density with lower than 85°C junction temperature². To achieve this goal, considerations on these aspects are necessary, and in fact they can be the weakness of cubic GaN LED. For instance, first principles calculation reveals that the thermal conductivity of cubic GaN is less than that of hexagonal GaN¹⁴ so that it might show a higher junction temperature. Similarly, as cubic GaN is grown on Silicon rather than conventional Sapphire substrate, we can expect lower light extraction than hexagonal GaN. Finally, as we have a wider quantum well, the transition from the conduction band to the 2nd heavy hole subband can be dominant depending on the injection level, making the peak wavelength blueshift. It is worth noting that due to the polarization and heavier transverse hole effective mass, 2nd heavy-hole subband transition is expected to be less dominant in hexagonal GaN LEDs even with the same quantum well thickness. Therefore, this spectrum issue should take current crowding into consideration, imposing at least 2D simulation to fully explore those LEDs. In short, 2D optical-thermal-electrical simulation is necessary for the exploration of cubic GaN LED, which deems this project pivotal for the realization of high WPE green LED.

This project composes of three parts. First, I will suggest the modeling of cubic GaN/InGaN material in Crosslight and simulate the basic stack design that is pre-optimized to show the appropriateness of my modeling and show the promise of cubic InGaN LEDs. Second, I will explore the optical-thermal-electrical aspects based on the conventional 2D LED design where we etch until the n-doped layer (n-GaN) to make an n-contact. Finally, I will suggest the vertical LED design that is feasible in GaN on Silicon and compare it with the 2D design.

II. Modeling of cubic InGaN/GaN in Crosslight

As it is challenging to grow pure cubic GaN, there are not so much experimental data that can be used for the simulation. Also, there are not so many variables built in the default macro. Therefore, appropriate modeling is necessary for the cubic InGaN/GaN simulation. Most of the parameters are either extracted

from the paper, or we are assuming the same value as that of hexagonal GaN, due to the scarcity of data. Most parameters (lattice constant, bandgap, spin-orbit splitting, electron-hole effective mass, Luttinger parameters, deformation potential, and elastic constants) are extracted from Vurgaftman et al.¹⁵ The Kane parameter is set to 0 due to the fact that the extracted Luttinger parameters are already modified, as the author says it is extracted from the calculation values of $m_{hh,z}$ and $m_{lh,z}$, which are already affected by the conduction band, by the following equations:

$$m_{hh,z} = \frac{1}{\gamma_1 - 2\gamma_2}$$

$$m_{lh,z} = \frac{1}{\gamma_1 + 2\gamma_2}$$

Otherwise, the Kane correction will make γ_2 negative, making the light hole mass heavier than the heavy hole mass. Setting the Kane parameter to 0 will underestimate the performance of cubic GaN LED, as it ignores the electron effective mass correction and uses the electron mass in the macro. Static dielectric constants are set as 9.7 for GaN and 15.3 for InN¹⁶, and the electron affinity is calculated by using the Model Solid Theory, neglecting the spin-orbit splitting and assuming linear interpolation in Valence Band Offset (VBO), while the VBO and base affinity are extracted from Y.C. Tsai and C. Bayram¹⁷. That is, electron affinity is calculated by:

$$\chi_{InGaN} = \chi_{GaN} + (E_{g,GaN} - E_{g,InGaN} - xVBO_{InN/GaN})$$

,where χ indicates electron affinity, E_g means the bandgap, and x means the mole fraction of Indium in InGaN. Donor and Acceptor activation energy is set as 30meV¹⁸, and 140meV¹⁹, respectively. Electron-hole mobilities are assumed to be the same as the Crosslight hexagonal GaN value, and the 300K ABC coefficients are assumed to be the same as hexagonal GaN from Y. C. Shen et al.²⁰ (18.5ns of SRH lifetime for both holes and electrons, and $C_n=C_p=10^{-30}$ cm⁶/s), as we do not have much experimental data for cubic GaN. This assumption underestimates the performance of cubic GaN, as we see from the point I made in the introduction. The radiative recombination coefficient at 300K for the bulk cubic GaN is assumed to be 3.2×10^{-11} cm³/s, which is calculated from the optical matrix element of cubic GaN theoretically. From these coefficients, bulk IQE can be calculated by:

$$\eta_{IQE} = \frac{Bnp}{\frac{n}{\tau_n} + \frac{p}{\tau_p} + Bnp + C_n n^2 p + C_p np^2}$$

, while the radiative recombination term (Bnp) is replaced by the spontaneous emission rate calculated from Fermi's golden rule to calculate the active region (quantum well) IQE. Linear interpolation in InGaN is assumed for almost all parameters except the bandgap and the affinity.

The modeling of raytracing is done following the examples in Crosslight. The metal was assumed non-transparent with a reflectivity value of 0.9 (Aluminium), and the surrounding material is air unless otherwise specified. The refractive index value is assumed to be 2.3 for GaN and 2.9 for InN, applying a linear interpolation for InGaN. This will lead to ~ 2.5 of the group index of the active region, as we will assume 33% of Indium content. We can calculate the theoretical extraction efficiency value for a single escape cone by the following equation:

$$\eta_{LEE} = \frac{1 - \sqrt{1 - \left(\frac{n_e}{n_s}\right)^2}}{2} \frac{4n_s n_e}{(n_s + n_e)^2} \frac{4n_e}{(n_e + 1)^2},$$

where n_s is 2.5 for our case and $n_e=1$ for no encapsulation, and $n_e=1.5$ for encapsulation. This equation gives us 3.4% of single-cone extraction for no encapsulation, and 9% of single-cone extraction for the epoxy-encapsulation case. This means that if we have light extraction from all 6 directions, we will have 6 times larger light extraction efficiency than the single-cone value. This will be the maximum achievable value considering only simple mechanisms, but multiple-reflected light can also be extracted, contributing to higher light extraction than the theory. While roughening or patterning of the surface is used to improve the light extraction in real devices, those methods are not considered in this project, meaning that we will be able to achieve further improvement with additional experimental methods.

Thermal properties are more challenging to model, as theoretical values and experimental values show large differences for hexagonal GaN also. Furthermore, the thermal conductivity value actually decreases as we make the film thinner²¹, and it has power-law dependence on the lattice temperature²². For the thermal conductivity, as it is expected that cubic GaN has near 3/5 of thermal conductivity value than hexagonal GaN, I used the same ratio from the default Crosslight value¹⁴. As hexagonal AlGaIn has a thermal conductivity value of 62 W/m-K (GaN has 130 W/m-K, but typically in Crosslight examples they use AlGaIn and set Al mole fraction to 0 to simulate GaN. It means that the thermal conductivity of GaN is typically 62W/m-K in Crosslight simulations) and thin-film InGaIn has thermal conductivity value of 10 W/m-K, my cubic InGaIn macro has a thermal conductivity of 37.2 W/m-K for the passive macro and 6W/m-K for the active macro. Also, for the power-law dependence, I used the same parameter as hexagonal GaN so that thermal conductivity decreases as temperature increases by an order of 1.3. Also, bandgap, carrier mobility, and SRH-Auger recombination coefficients also change with temperature. Bandgap parameters are extracted from Vurgaftman et al.¹⁵. For the carrier mobilities, the same value as hexagonal GaN is used. For SRH and Auger recombination coefficients, only the ratio of values between different temperatures are extracted²³ and applied to the base value we have at 300K. For the radiative recombination, the power law of 1.5 is used from the 300K value²³. For the heat escape, I used the common assumption that is used for Crosslight hexagonal GaN LED simulation, except for the special case: heat can only escape through the n-contact with the 2D thermal conductance value of 200. (W/m-K) In this way, optical-thermal-electrical modeling of cubic InGaIn was complete.

The base stack of this study is shown in Figure 1 (a). On top of 120nm n-type GaN, 5nm single Quantum Well with 14nm Barrier is grown. And then, 100nm p-type GaN is grown, and 15nm p+ GaN for the ohmic contact and the current spreading concludes the structure. A single Quantum Well structure is simulated because the Auger recombination inside the cubic GaN is expected to be low due to the absence of polarization²⁴, resulting in low efficiency droop even for a single quantum well. Mg doping is one order higher than the Si doping to compensate for the activation energy asymmetry between Mg and Si. 5nm Quantum Well thickness in this structure has two reasons. First, it is widely accepted that a wider quantum well has higher IQE in LEDs without polarization due to the increase of active volume.²⁵ Preliminary simulations also reveal that the IQE generally goes higher as we make the quantum well thicker. However, as we have a thicker Quantum Well, we cannot ignore the transition from the conduction band to the 2nd heavy-hole band. This transition is actually injection level dominant, and I found out that 6nm of Quantum Well has a shorter peak wavelength at 100A/cm² due to the comparable intensity of both transitions: C-HH1 and C-HH2. This is the reason why I chose 5nm of Quantum Well thickness. Figure 2 (b) shows the IQE curve of the designed stack and Figure 2 (c) shows the Electroluminescence (EL) spectrum of the designed stack at the current density of 100A/cm² when simulated with the 1D structure where we have n-contact at the bottom and p-contact at the top. The broadening factor used in EL spectrum is the default value of Crosslight. It clearly shows ~84% of IQE

and ~540nm of peak emission wavelength at 100A/cm², showing the superior performance of cubic GaN green LED over its hexagonal counterpart.

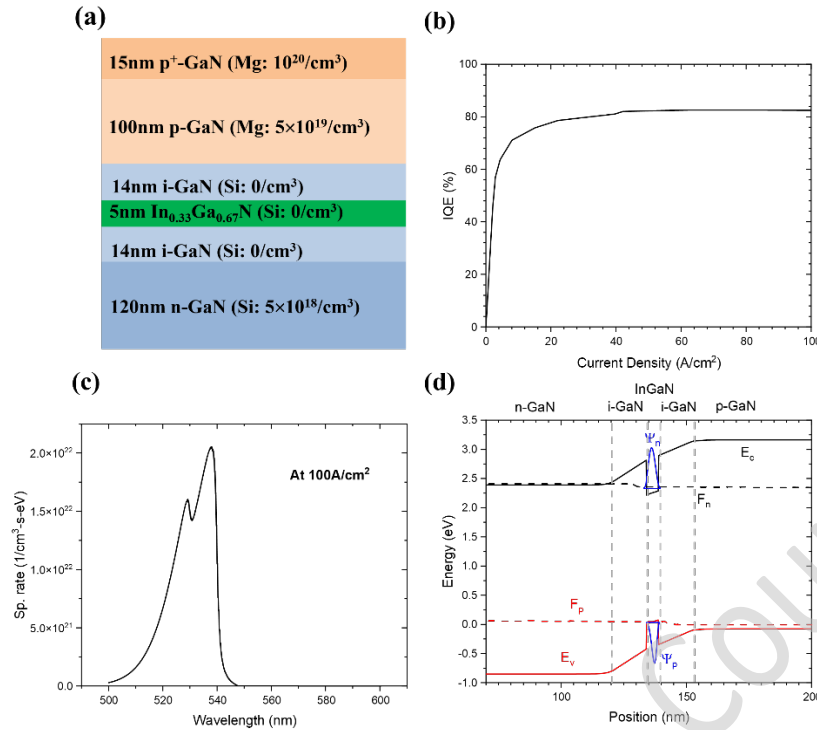


Figure 1. (a) The 1D SQW stack as a basis, (b) Its IQE curve, (c) The EL spectrum at 100A/cm², and (d) the band structure of the single quantum well at 100A/cm². Only ground states are shown in the band structure.

In order to check the validity of this thermal modeling in the bandgap, recombination coefficients, and other parameters, the simulation of the same structure without heat flow, while assuming constant lattice temperature, was conducted. The results are shown in Figure 2. In Figure 2 (a), we can clearly see the decrease in IQE due to the decrease in SRH recombination lifetime and the increase in Auger recombination coefficient, as we increase the temperature. In Figure 2 (b), the redshift in the spectrum is observed due to the bandgap narrowing effect of temperature.

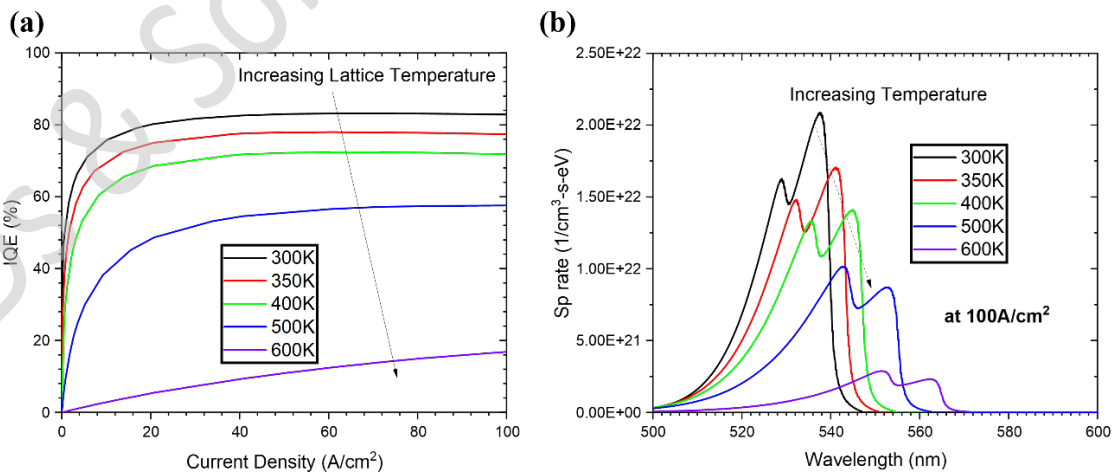


Figure 2. (a) IQE-curve (b) EL spectra at 100A/cm² for various lattice temperatures.

III. Conventional “on wafer” 2D Structure of cubic GaN LED

Based on the stack suggested in section 2, conventional 2D structure is simulated, assuming that we have an additional 500 μm Silicon substrate and 500nm intrinsic GaN, accounting for the layers in the actual sample. Assuming we dry-etch until n-GaN and put the n-contact therein, 300 μm of mesa size is assumed, and the whole mesa is simulated, while the half structure is shown in Figure 3 (a), as the structure is symmetric. Here the metal width is assumed to be L. Perfect passivation is assumed so that we do not have surface recombination or traps at the sidewall. The common issue in these 2D LED is the current crowding, culminating in increased efficiency droop than the current-spread case. In cubic GaN LED, current crowding also results in decreased IQE, as no LEDs are completely droop-free. However, the current crowding is also a serious issue in cubic GaN LED, contrary to conventional beliefs: the light extraction, lattice temperature, and the peak wavelength are all affected by the current crowding. First, light extraction is affected by the current crowding because the Silicon substrate is absorptive. That is, if the current is not spread enough, most of the light is generated “underneath” the metal contact: among the six escape cones, light through the top cone will be reflected by the metal and light through the bottom cone will be absorbed by the substrate. The other 4 escape cones will not enhance the extraction much due to the photon recycling in the active region. Similar points are made for III-Phosphide red LEDs, where the substrate is absorptive GaAs²⁶. Therefore, current crowding will lead to extremely low light extraction for cubic GaN LEDs on Silicon. Second, lattice temperature tends to increase when the current is crowded, as the temperature can increase more if the heat source is focused on a certain area. Also, IQE in a certain area does decrease when the current is crowded, exceeding near 500A/cm², leading to more non-radiative heat sources than the current spread case. Therefore, current crowding will also lead to higher junction temperature, deteriorating the performance of cubic GaN LED. Finally, peak wavelength will decrease, aside from the increase due to increased temperature, due to the dominance of higher heavy-hole band transition. This occurs due to carrier overflow in high injection levels. This will lead to a design limitation where we might have to increase the indium content further or decrease the quantum well thickness, compromising the IQE due to either high defectivity or thinner active regions.

Considering the abovementioned reasoning, the optimization of the 2D structure should be focused on how we can reduce the current crowding. First, the ohmic contact width L was changed to research its effect on the current spreading. The current is simulated until 300A/m, so that it corresponds to 100A/cm² when it is spread all along with the 300 μm of mesa length. Figure 3 (b) shows the +y direction current density inside the quantum well as a function of horizontal position from the center. The position of 150 μm indicates the right sidewall in Figure 3 (a). If we assume perfect current spreading, the value should be -100A/cm² for all positions. Conventional belief is that the wider the ohmic contact, the better the current spreading, and it seems to be true, although the maximum y-direction current density is the highest in metal-all-over case. This can be explained by the following reasonings: In this simulation, the current follows the shortest path to minimize the resistance. Therefore, most of the current flows through the edge of the contact to take the shortest path to the n-contact, with a certain amount of spreading based on the p-GaN layer hole mobility. As we are currently assuming the same mobility with hexagonal GaN and cubic GaN is expected to have better hole mobility⁸, it is worth noting that we are overestimating the current crowding than the real case. Furthermore, we are not considering any band bending on the sidewall, whether it is due to the sidewall passivation or the surface states. Although this simulation is somewhat over-estimating the current crowding, it is still pivotal to see the downsides of the current crowding in cubic GaN green LEDs. In this regard, the abovementioned overall side-effect of current crowding is shown in Figure 4. Figure 4 (a) shows that Light Extraction Efficiency (LEE) is extremely low (~0.4%), except for L=300 μm case, because the current is not spread enough. A sudden increase in LEE to ~3% at L=300 μm is due to the additional escape of the light from the right sidewall, as most of the recombination occurs near the sidewall. Figure 4 (b) shows that the temperature increases as the ohmic contact becomes narrower, although it is not clear whether it is solely the effect of current crowding at this point: it is possible that the heat source moved more closer to the n-contact, leading to

lower temperature because the heat can escape through the n-contact more easily. Nevertheless, the maximum temperature (probably junction temperature) is lower than 85°C in all cases, which is hopeful for the realization of cubic GaN LEDs. However, Figure 4 (c) shows that current crowding is not solved in all five cases, as the spectra still show ~520nm of peak emission wavelength.

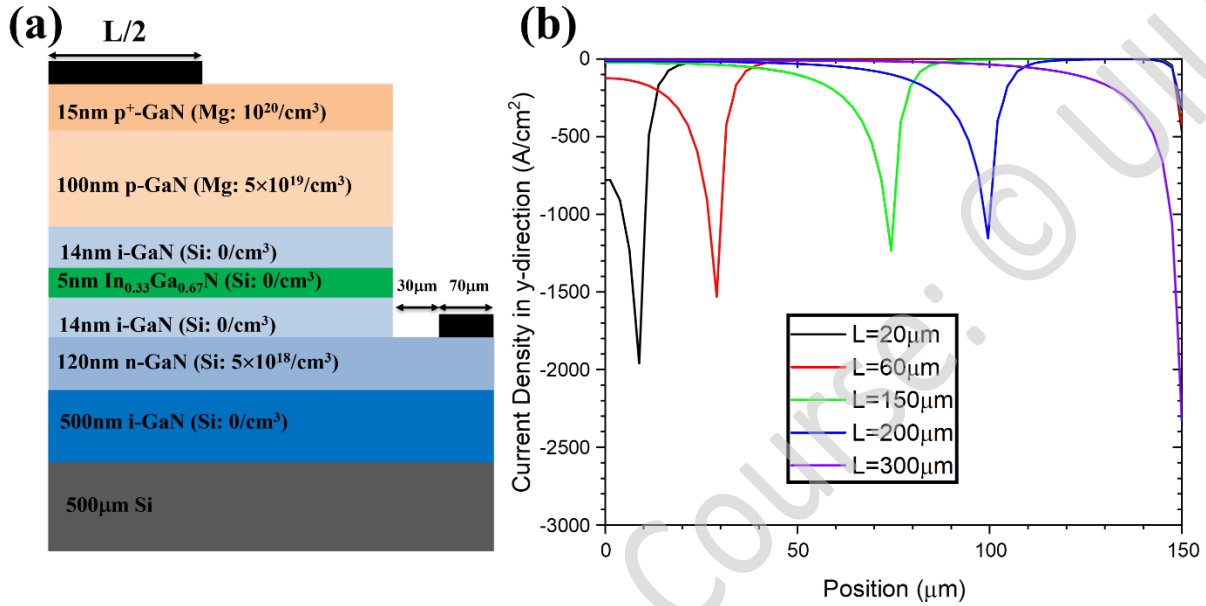


Figure 3. (a) The simulated base structure for 2D LED (b) y-direction current density inside the active region with respect to horizontal position. It shows the point where the current crowding occurs.

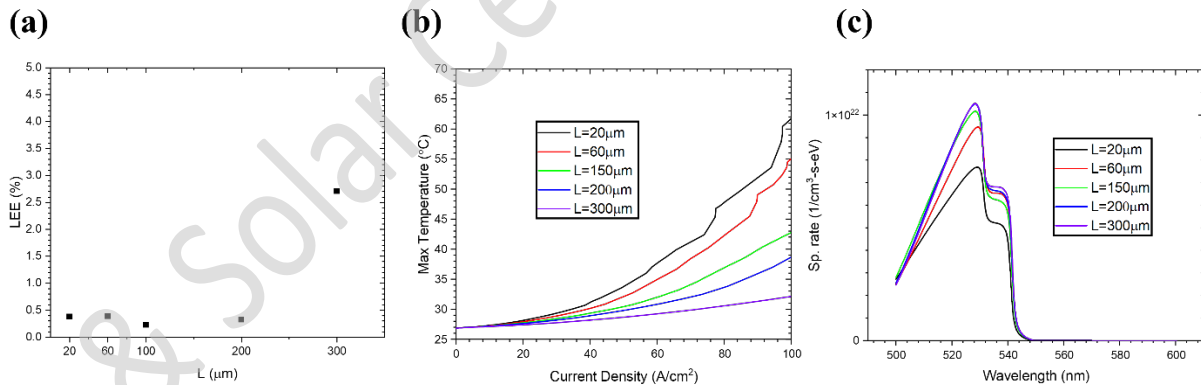


Figure 4. (a) The Light Extraction Efficiency (LEE) at 100A/cm², (b) The maximum Temperature as a function of current density, and (c) EL spectra at 100A/cm², with various ohmic contact widths.

Most of the common solution for the current crowding is to apply a current spreading layer such as Indium Tin Oxide (ITO)²⁷. This role of ITO cannot be replaced by thicker p⁺ GaN, as the hole mobility in p⁺ GaN is restricted and their resistivity is higher than the ITO. However, optimum ITO thickness will exist in this case, as thick enough ITO will be equivalent to the ohmic contact that is 300µm wide, and most of the current will flow through the sidewall as we see in Figure 3 (b) L=300µm case. In this regard, the simulation to determine the optimal thickness of ITO was conducted. ITO was assumed on top of p⁺ GaN layer, and the metal contact width L is assumed to be L=100µm. The results are shown in Figure 5.

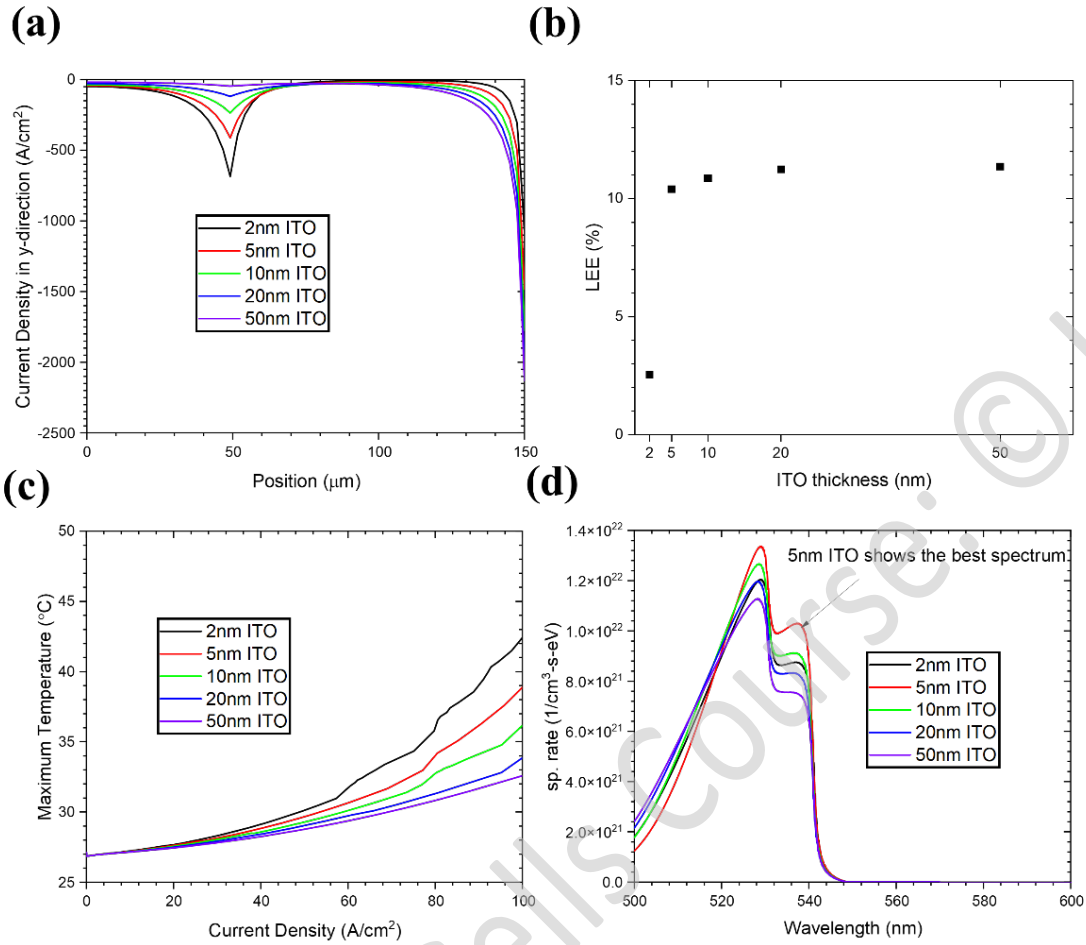


Figure 5. (a) The y-direction current density in the active region, (b) Light Extraction Efficiency at 100A/cm², and (c) EL Spectra at 100A/cm² are plotted at various ITO thicknesses.

From Figure 5 (a) and Figure 5 (d), it can be concluded that 5nm ITO shows the best current spreading result. Of course, thin ITO has experimental issues such as bad crystal quality. I ignored those considerations in this simulation. With improving the current crowding, the LEE also improved due to the fact that generated light is not “blocked” by the metal contact. Also, sidewall light extraction may also have taken place, as we see that most of the recombination occurs at the sidewall. Now the device shows desirable ~10% of on-wafer LEE, but the spectrum issue is not solved, from Figure (d).

Considering the fact that current spreading in fact depends on the resistivity of each layer, the possible solution is to have high conductivity layer below the n-GaN, or increase the thickness of n-GaN to prevent the early-stage current crowding at the sidewall. That is, if we have low resistivity path that passes through the high conductivity layer, they will not be crowded at the sidewall. As a demonstration, I tried to change the Silicon doping level instead. Figure 6. (a) shows the effect of Silicon doping on the current spreading when we have 5nm ITO atop p+ GaN. As we increase the Silicon doping, we can see that the current is more spread because now the current passes through the Silicon substrate, preventing the early-stage current crowding at the sidewall. Here, L is assumed to be L=100μm. We can see that the intensity of the transition from the conduction band to the first heavy hole subband is restored. Further current spreading is expected to occur by using the wider contact or applying ITO. However, another solution to this current crowding is moving into vertical LED structure, and I will move into this topic, rather than continue exploring 2D LEDs.

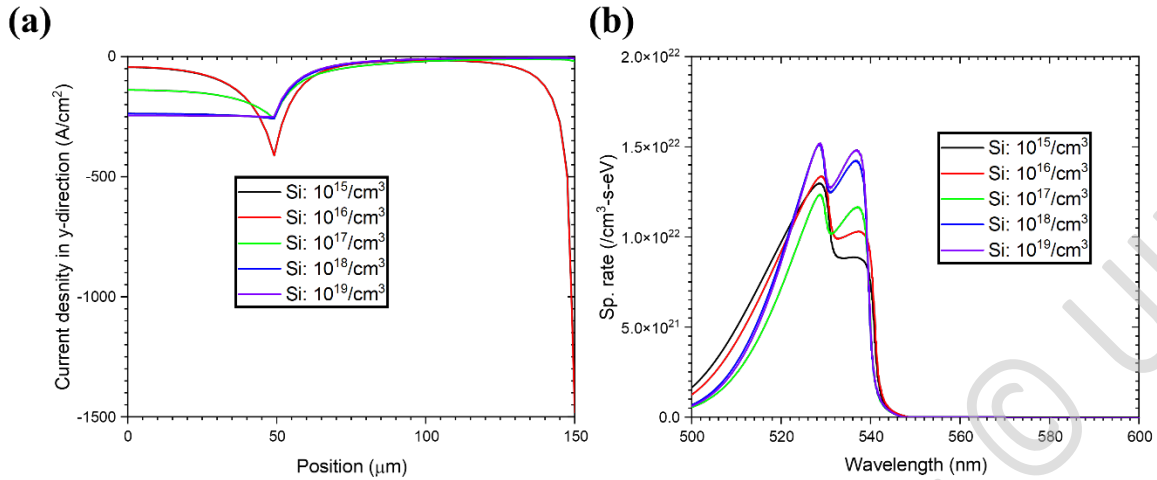


Figure 6. (a) y direction current density distribution in the active region, and (b) EL spectra at $100\text{A}/\text{cm}^2$, at various doping levels for Silicon.

IV. “On-wafer” vertical cubic GaN LED

There is an interesting idea of vertical LED, rather than the conventional 2D LED²⁸. It has better current spreading than 2D LED structure, which is exactly needed in this case. Furthermore, whereas vertical LEDs typically exhibit higher cost due to extra fabrication steps (especially, substrate removal is necessary for GaN on Sapphire as Sapphire is not so conductive,) cubic GaN LED on Silicon can even make an “on-wafer” vertical LED thanks to the conductive, Silicon substrate if we use adequate doping level. Also, the removal of Silicon will be easier than the conventional method we use (laser lift-off, chemical lift-off, etc.) The basis structure for this simulation is suggested in Figure 7 (a). Compared to the previous structure, the Silicon and the i-GaN layer is now doped to provide enough conductivity for the vertical LED. In fact, the doping level for the Silicon here is a little low. However, it does not affect the optical properties of the device. Another thing to note is that the thermal simulation of this device shows a thermal runaway issue, as the heat should pass through $500\mu\text{m}$ of substrate layer before it can escape through the n-contact. This can be seen in Figure 7 (b), where we have a huge thermal gradient all over the Silicon substrate. In this regard, before the removal or the spalling of Silicon substrate, the thermal simulation is disabled to only research the electrical and optical aspects of on-wafer vertical LEDs. In fact, if I assume that we can reduce the thickness of the Silicon by physical spalling, making the Silicon thickness to $20\sim 200\mu\text{m}$ makes the maximum temperature $29\sim 60^\circ\text{C}$, proving that this thermal runaway is due to Silicon. We can expect less issue in real on-wafer vertical LEDs, as our assumption that the heat only escapes through the n-contact is an aggressive assumption: it is assuming the worst case.

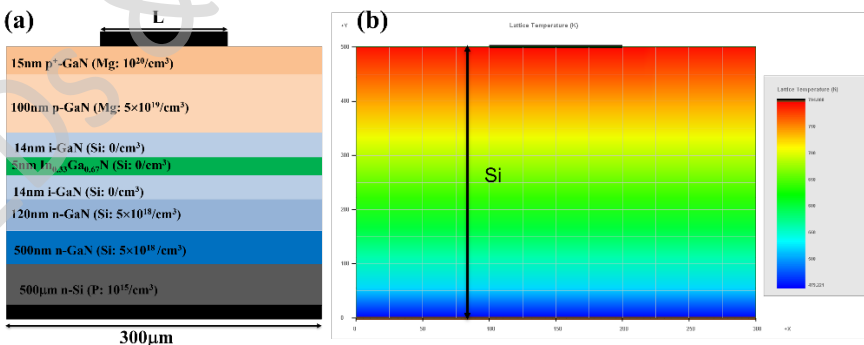


Figure 7. (a) Vertical LED Structure, and (b) the Temperature mapping showing the thermal runaway issue

Without considering the thermal aspect, the y direction current density inside the active region, and the EL spectra at $100\text{A}/\text{cm}^2$ are shown in Figure 8. We can now see that perfect current spreading can be achieved if we have ohmic contact (p-contact) all over the mesa. Furthermore, Figure 8 (b) shows that we can restore $\sim 540\text{nm}$ of peak wavelength if we have large enough p-contact width. It clearly proves that vertical LED can solve the current crowding issue very easily.

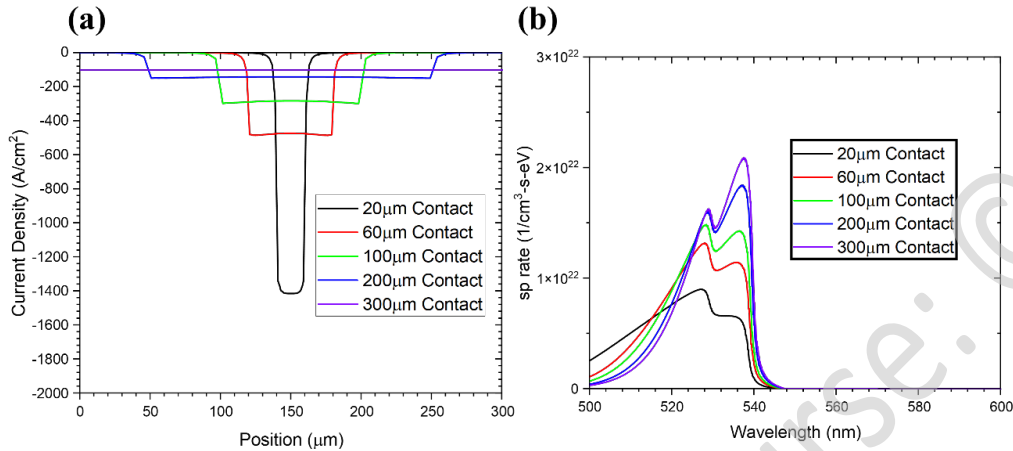


Figure 8. (a) y direction current density inside the active region, and (b) EL spectra at $100\text{A}/\text{cm}^2$, with various metal contact width

As this device shows $0.0006\sim 0.01\%$ of LEE because most light rays are generated underneath the metal contact, further improvement in current crowding and LEE can be made by applying ITO on top of the p+ GaN layer, similar to the 2D LED case. However, as ITO is still absorptive, optimal thickness of ITO will exist that provides decent current spreading and decent transparency. For the strict optimization, various combinations of metal width and ITO contact were tested. For each metal width, the ITO contact that gives maximum External Quantum Efficiency (EQE), the product of IQE and LEE, was chosen. The results are shown in Figure 9. The max EQE was achieved when we have $100\mu\text{m}$ contact and 75nm of ITO, resulting in 82.23% of IQE and 7.99% of LEE. (e.g., 6.57% of EQE) Figure 9 (a) shows the maximum achievable EQE when changing the ITO thickness for each metal contact width, and Figure 9 (b) shows the y direction current density when we have $100\mu\text{m}$ metal and 75nm ITO: the optimal case. The spontaneous emission spectrum (not shown here) still shows $\sim 540\text{nm}$ of peak emission wavelength, indicating the extent of current spreading shown in Figure 9 (b) is enough.

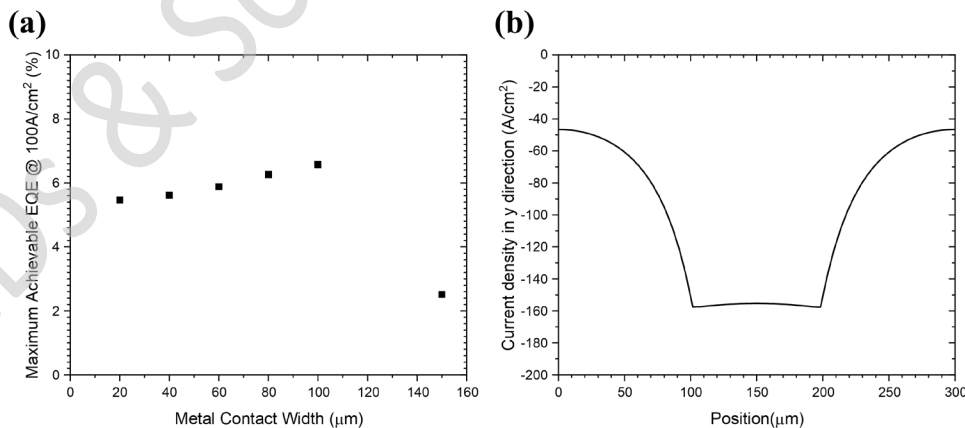


Figure 9. (a) Maximum achievable EQE at $100\text{A}/\text{cm}^2$ for each metal contact width. (b) The extent of current spreading with $100\mu\text{m}$ metal and 75nm ITO, $100\text{A}/\text{cm}^2$.

Although this ITO-approach is effective, a significant portion of the light is absorbed by the contact. In this regard, if we use transparent contact instead of opaque contact and ITO, it will further increase the LEE. Fortunately, annealing the Ni/Au contact will give transparent p-contact with the Transmittance of 60~88%²⁹. Using the 83% Transmittance value from the paper, 50nm transparent contact with the refractive index of $2+i0.155$ is used so that only 17% of power is absorbed during one pass. The simulation demonstrated that the LEE is nearly irrelevant to metal contact width if we apply transparent annealed Ni/Au contact. The maximum EQE of ~8.7% was obtained for 300 μm wide transparent contact. The simulated EQE curve for this device is shown in Figure 10. We must consider the fact that we are running 2D raytracing, so further studies might reveal different LEE values.

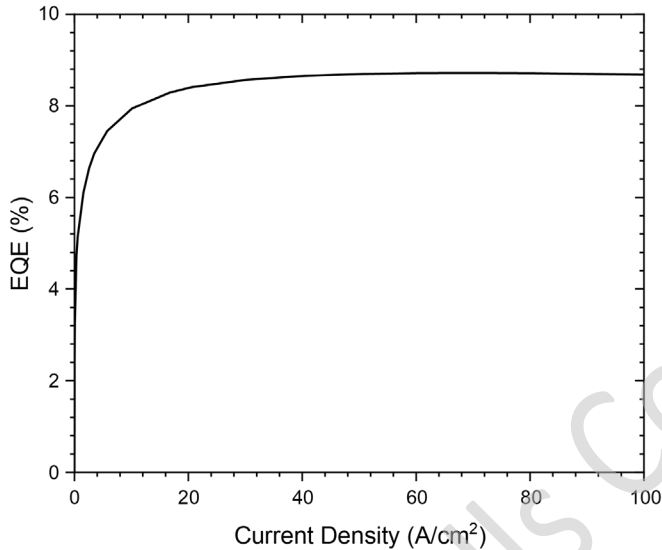


Figure 10. EQE curve of the on-wafer vertical LED with transparent annealed Ni/Au contact

V. Substrate Removal and Flip-Chip Bonding / Encapsulation

So far, we have explored two on-wafer solutions. As the Silicon substrate is relatively easy to remove, and the substrate is absorptive, we can further improve the EQE by flip-chip bonding the LED to another die and removing the Silicon substrate. 2D LEDs have some extent of current crowding at the sidewall, so they are only explored at the end of this section with the solution of thick doped n-GaN at the bottom, which might lead to higher defectivity in the experimental perspective. Therefore, this section will mainly focus on vertical LED structure, which is a viable design for cubic GaN on Silicon. The basis structure for this simulation is shown in Figure 11 (a). Now, we assume that the heat sink/driver is connected to the p-contact, and we have to make the p-contact with a reflective metal so that the light is not absorbed into the driver substrate. ITO can be moved into the region between the n-contact and the n-GaN, and Silicon is completely removed. The light will be extracted in -y direction, rather than +y direction. Also, to simulate the actual LED chip, I assumed encapsulation with the epoxy refractive index of 1.5. The dome-shaped encapsulation was assumed to have 110 μm height and 500 μm radius. In the first simulation, L is assumed to be L=100 μm , which produces the best result for on-wafer LEDs. Figure 11 (b) shows the EQE at 100A/cm² as a function of ITO thickness, assuming L=100 μm . The maximum EQE turned out to be ~16% (LEE of ~20%) when the ITO thickness is 90nm. This is nearly 2.5 times improvement with the same metal contact width compared to the on-wafer solution.

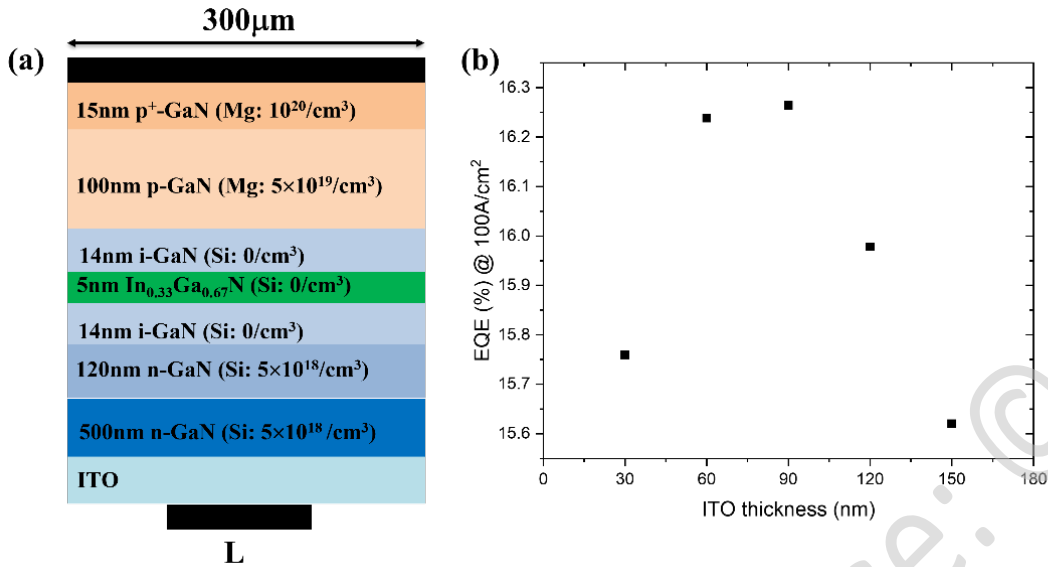


Figure 11. The reversed schematic of the Flip-Chip Vertical LED design. P-contact is connected to the heat sink/driver

Changing the metal width L , it turned out that for Flip-Chip LEDs with encapsulation, narrow metal with thick ITO shows higher EQE value. It can be accounted for by the increase in the critical angle due to the encapsulation. Therefore, more lights are obscured by the metal if the metal is wider. The simulation result for $L=20\mu\text{m}$ is shown in Figure 12 (a).

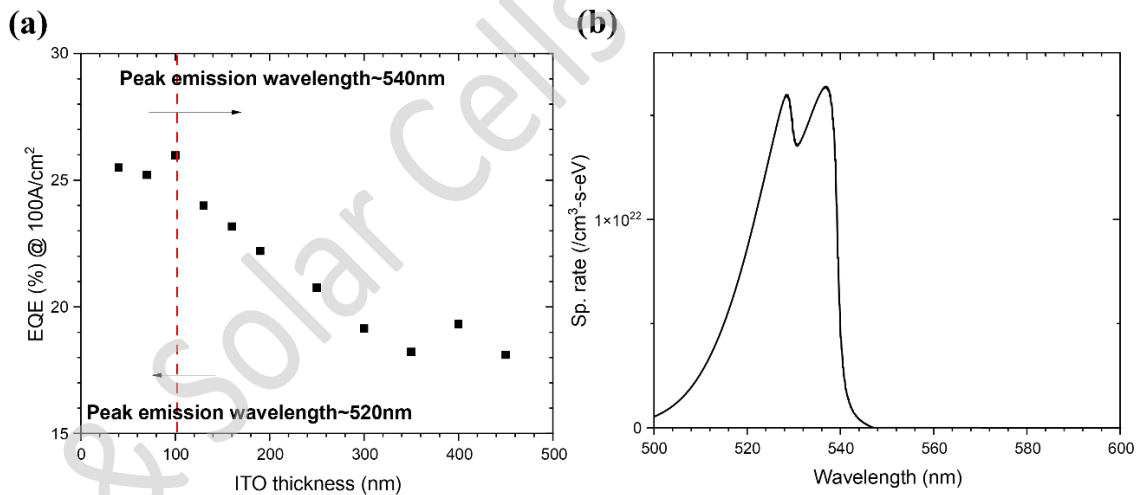


Figure 12. (a) EQE at 100A/cm² as a function of ITO thickness when $L=20\mu\text{m}$ (b) EL spectrum when ITO is 130nm thick.

Now, it turned out that as our contact width is narrow, it is more sensitive to current crowding and ITO thickness. Taking it into consideration, the maximum EQE at 100 A/cm² while maintaining $\sim 540\text{nm}$ of emission wavelength turned out to be $\sim 24\%$, which is similar to our target: 30% EQE. The EL Spectra of the corresponding case is shown in Figure 12 (b). However, wire-bonding to the $20\mu\text{m}$ contact might be challenging in an experimental perspective.

In this regard, flip-chip encapsulated LED with Ni/Au transparent metal contact is simulated as a final and optimized attempt, where we remove the ITO and cover the whole mesa with the transparent contact.

Also, assuming that we are using silver bonds, the improved reflectance value of the p-contact was assumed: 0.95. In order to check whether this device fulfills the DOE criteria², the schematic of the device, JV curve, spectrum, junction temperature, EQE curve, and WPE curve are shown all together in Figure 13.

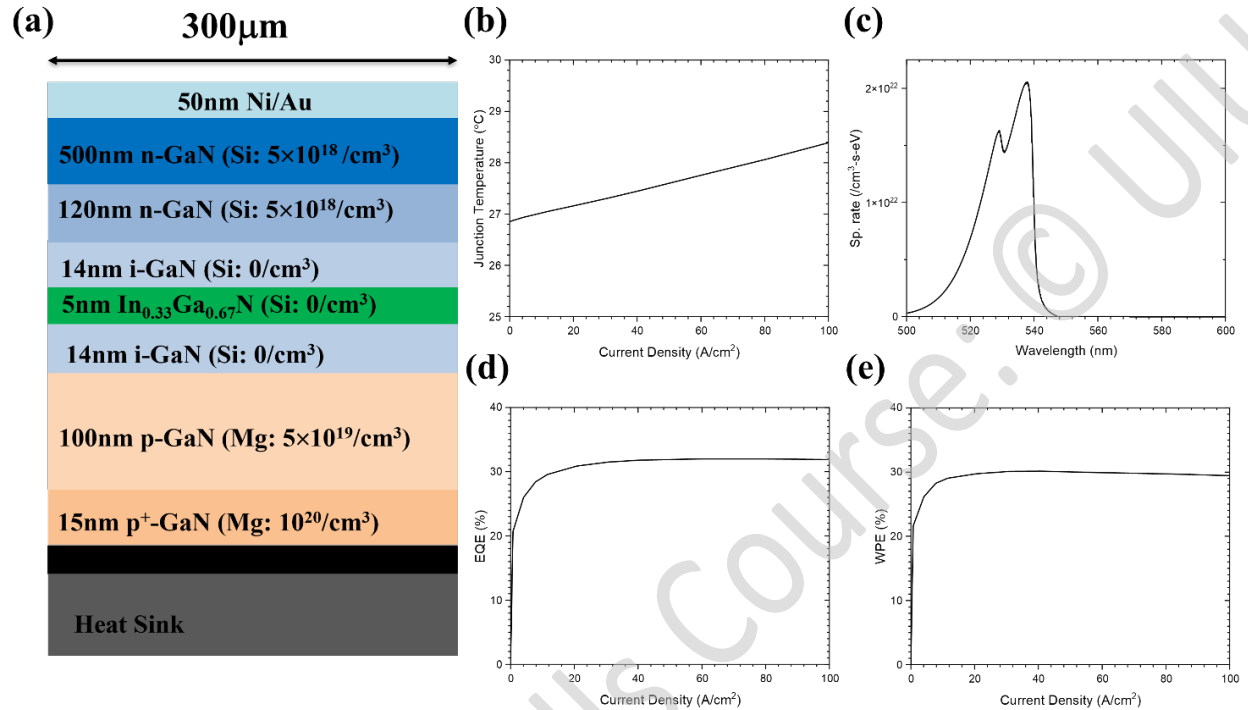


Figure 13. (a) Schematic of Flip-Chip LED with transparent Ni/Au contact, (b) junction temperature as a function of current density, (c) EL spectrum at 100A/cm², (d) EQE curve, and (e) WPE curve.

The simulation result shows that with the Flip-chip vertical LED that utilizes transparent contact and a highly reflective bond, we can fulfill DOE 2025 target for the green LED (~30% WPE @ 100A/cm² with junction temperature less than 85°C.) It is especially hopeful in that I had some extreme assumptions (e.g., significantly low thermal conductivity, higher Auger loss than that predicted in theory, etc.) I did not implement any roughening or light extracting features in my simulation. Particularly, cubic GaN on nanopatterned Silicon (100) usually has patterns that can remain even after hexagonal GaN removal, attributing to the light extraction. If we take into consideration any light extracting method, the LEE can be higher than the current ~38.9% of LEE, which opens the possibility of extremely power-efficient green LEDs for the SSL. Another interesting and worth-noting point is that comparing Figure 13 (d) and (e), we can see that EQE and WPE do not have much difference: it is predicted from the absence of polarization, since in hexagonal GaN green LEDs, polarization and the Electron Blocking Layer itself acts as an injection barrier, increasing the forward voltage and decreasing the WPE, compared to EQE. This brings light to another superior aspect of cubic GaN LED: it is easier to convert EQE directly into WPE, while normally the inequality $WPE \leq EQE < IQE$ holds.

Finally, I would like to briefly mention the Flip-chip simulation results for 2D LED structure. Here, heat is assumed to escape through both n and p contact with the 2D thermal conductance of 200 W/m-K, which are connected to the heat sink. The same encapsulation as the vertical flip-chip case is assumed, and the metal contacts now cover the entire mesa and the n-region, so that it can reflect the light going in the heat sink direction. Reflectance of both contacts are assumed to be 0.95, assuming opaque metal. I

assumed that we grow $10\mu\text{m}$ highly doped ($5\times 10^{20}/\text{cm}^3$) n-GaN atop Silicon and then start to grow the epi-layer, removing the Silicon later for the flip-chip design. I chose this doping level to demonstrate the current spreading, but lower doping will also work, given that the layer is thick enough. The simulation results are shown in Figure 14.

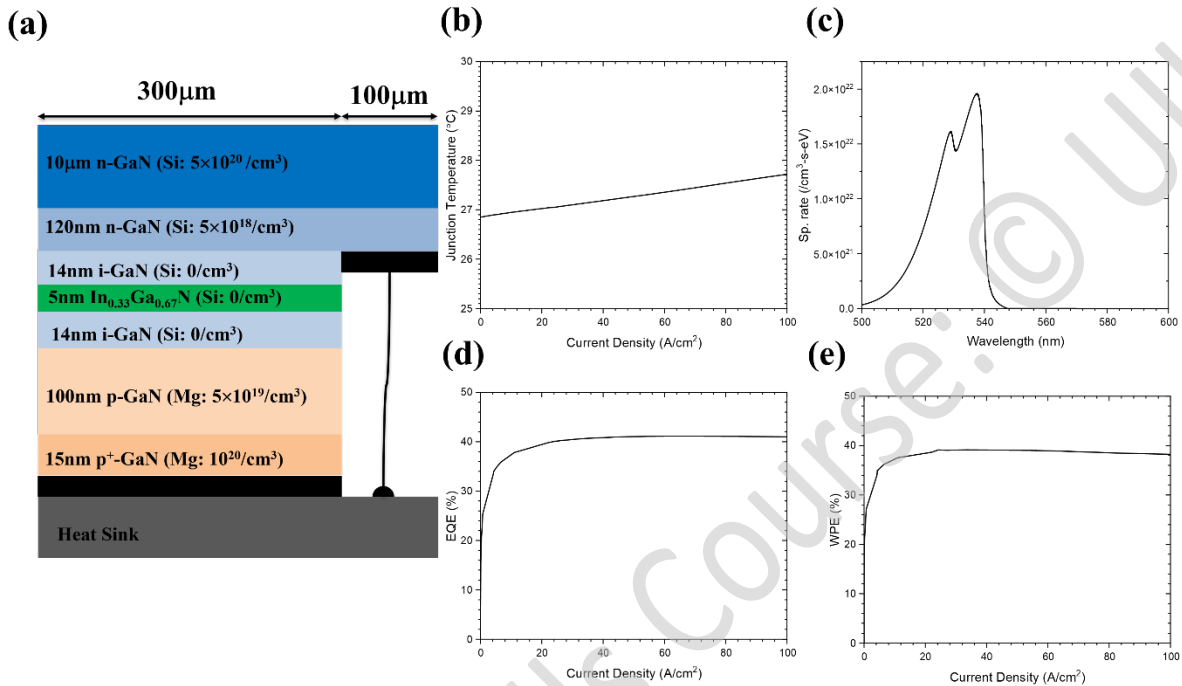


Figure 14. (a) Flip-chip 2D LED design, and its simulation results: (b) junction temperature, (c) EL spectra at $100\text{A}/\text{cm}^2$, (d) EQE, and (e) WPE.

It shows decent current spreading, as seen from Figure 14 (c). Indeed, it shows higher LEE ($\sim 50\%$) and therefore higher EQE ($\sim 40\%$) than the vertical flip-chip LED case. This data can be explained by the sidewall current crowding: although both LEDs have some extent of current crowding, current crowding in vertical LEDs occur at the center, while current crowding in 2D LEDs occur at the edge. Therefore, more light is generated from the edge of the LED in 2D LED case, and the light created from the edge can be easily extracted from the sidewall, as it has low probability of photon recycling. This is precisely the same reason why micro LEDs should show higher LEE in theory. Of course, it needs caution since we are assuming no surface traps and no band bending effect from the surface passivation. In reality, current crowding at the edge is not beneficial because the sidewall is the area that is most damaged by the dry etch process. Therefore, current crowding at the edge will result in lower IQE and lower performance, unless it is properly tackled by the passivation.

Nevertheless, it shows that we have a way to utilize 2D cubic GaN green LED as a flip-chip and successfully overcome the current crowding issue, given that we overcome the crystal quality issue from growing thick highly doped layer and the surface damage from the dry etch.

VI. Conclusion

In short, I realized the 2D optical-thermal-electrical simulation via Crosslight by carefully choosing the parameters and implementing experimental data and models. Using these parameters, I simulated cubic GaN LED on Silicon in the green wavelength region and tried to explore the area that can be a weakness of cubic GaN LEDs, compared to their hexagonal counterparts. In this process, I found out that current crowding is a pivotal issue in cubic GaN LEDs (especially for wide quantum well LEDs,) and we can solve it by using vertical LEDs. Furthermore, we can improve the EQE of the vertical LED from ~9% to ~32% by flip-chip bonding the vertical LED to another substrate and removing the absorptive substrate. When we use non-transparent ohmic contact and ITO, the change is from ~6.5% to ~16%. We can further improve this value by introducing roughening or other light extraction features, which are not considered in this project. Also, the simulation for flip-chip bonding of the 2D LED structure has also been suggested, despite expected experimental difficulties, showing similar or higher light extraction due to the sidewall emission and the solved current crowding issue. The light extraction efficiency value presented in this work does not surely hold the exact value as it is based on 2D simulation (not 3D) and the parameters used might be different from the real case, but this project has three pronounced significances. First, it shows us the approximate improvement we can get when we remove the substrate so that we can predict off-wafer EQE from on-wafer EQE values. Second, it shows that approximately we can meet the DOE 2025 goal for green LEDs with cubic GaN LED on Silicon without any further engineering, thereby proving the promise of cubic GaN LED: it will show much higher value if we consider other technologies in the encapsulation. Finally, it deals with the possible issue other than IQE when we actually make a device from cubic GaN on Silicon, which was not dealt with before, to my knowledge.

Further improvements to this project can be made by moving into 3D simulations. It will be a significant computational burden since optical-thermal-electrical simulation itself requires self-consistency among many equations in different categories. However, further progress in 3D simulation may enable two new exploration schemes: the way to reduce the current crowding in conventional 2D LED structure by the ohmic contact design, and more precise light extraction efficiency calculation for improved prediction and decision making. Furthermore, the way to further increase the LEE of vertical flip-chip LEDs can also be determined.

Another further topic of study is how we can reduce the current crowding of flip-chip 2D LED by adding a high conductivity layer on the bottom of the layer. For instance, we can increase the thickness of the n-doping GaN layer so that we can increase the current spreading, as shown in section V.

VII. Reference

- ¹ S. Nakamura, T. Mukai, and M. Senoh, "Candela-class high-brightness InGaN/ AlGaIn double-heterostructure blue-light-emitting diodes," [Applied Physics Letters 64 1687 \(1994\)](#).
- ² DOE BTO Solid-State Lighting Program, ["2022 DOE SSL R&D Opportunities."](#)
- ³ M. A. Maur, A. Pecchia, G. Penazzi, W. Rodrigues, and A. D. Carlo, "Efficiency Drop in Green InGaN/GaN Light Emitting Diodes: The Role of Random Alloy Fluctuations," [Physical Review Letters 116 027401 \(2016\)](#).
- ⁴ G. Lheureux, C. Lynsky, Y.-R. Wu, J. S. Speck, and C. Weisbuch, "A 3D simulation comparison of carrier transport in green and blue c-plane multi-quantum well nitride light emitting diodes," [Journal of Applied Physics 128 235703 \(2020\)](#).
- ⁵ K.T. Delaney, P. Rinke, and C.G. Van de Walle, "Auger recombination rates in nitrides from first principles," [Applied Physics Letters 94 191109 \(2009\)](#).
- ⁶ J. Simon, N.T. Pelekanos, C. Adelman, E. Martinez-Guerrero, R. André, B. Daudin, L.S.Dang. and H. Mariette, "Direct comparison of recombination dynamics in cubic and hexagonal GaN/AlN quantum dots," [Physical Review B 68 035312 \(2003\)](#).
- ⁷ M. Suzuki and T. Uenoyama, "First principles calculation of effective mass parameters of GaN," [Solid-State Electronics 41 \(2\) 271 \(1997\)](#).
- ⁸ C.A. Hernández-Gutiérrez, Y.L. Casallas-Moreno, V.-T. Rangel-Kuoppa, D. Cardona, Y. Hu, Y. Kudriatsev, M.A. Zambrano-Serrano, S. Gallardo-Hernandez, and M. Lopez-Lopez, [Scientific Reports 10 16858 \(2020\)](#).
- ⁹ <https://www.kubos-semi.com/about-kubos>
- ¹⁰ R.M. Kemper, M. Weigl, C. Mietze, M. Haberen, T. Schupp, E. Tschumak, J.K.N. Lindner, K. Lischka, and D.J. As, "Growth of cubic GaN on nano-patterned 3C-SiC/Si (001) substrates," [Journal of Crystal Growth 323 84 \(2011\)](#).
- ¹¹ A. Gundimeda, M. Frentrup, S.M. Fairclough, M.J. Kappers, D.J. Wallis, and R.A. Oliver, "Investigation of wurtzite formation in MOVPE-grown zincblende GaN epilayers on Al_xGa_{1-x}N nucleation layers," [Journal of Applied Physics 131 115703 \(2022\)](#).
- ¹² C. Bayram, J.A. Ott, K.-T. Shiu, C.-W. Cheng, Y. Zhu, J. Kim, M. Razeghi, and D.K. Sadana, "Cubic Phase GaN on Nano-grooved Si (100) via Maskless Selective Area Epitaxy," [Advanced Functional Materials 24 \(28\) 4492 \(2014\)](#).
- ¹³ D. R. Elsaesser, M. T. Durniak, A. S. Bross, and C. Wetzel, "Optimizing GaInN/GaN light-emitting diode structures under piezoelectric polarization," [Journal of Applied Physics 122 115703 \(2017\)](#).
- ¹⁴ D.-S. Tang, and B.-Y. Cao, "Phonon thermal transport properties of GaN with symmetry-breaking and lattice deformation induced by the electric field," [International Journal of Heat and Mass Transfer 179 121659 \(2021\)](#).
- ¹⁵ I. Vurgaftman and J. R. Meyer, "Band parameters for nitrogen-containing semiconductors," [Journal of Applied Physics 94\(6\) 3675 \(2003\)](#).
- ¹⁶ M. E. Levinshtein, S. L. Rumyantsev, and M. S. Shur, "*Properties of Advanced Semiconductor Materials: GaN, AlN, InN, BN, SiC, SiGe*," [John Wiley & Sons. \(2001\)](#).
- ¹⁷ Y.-C. Tsai and C. Bayram, "Band Alignments of Ternary Wurtzite and Zincblende III-Nitrides Investigated by Hybrid Density Functional Theory," [ACS Omega 5 3917 \(2020\)](#).
- ¹⁸ U. Birkle, M. Fehrer, V. Kirchner, S.Einfeldt, D. Hommel, S. Strauf, P. Michler, and J. Gutowski, "Studies on Carbon as Alternative P-Type Dopant for Gallium Nitride," [Materials Research Society Internet Journal of Nitride Semiconductor Research 4 S1 G 5.6 \(1999\)](#).
- ¹⁹ F. Mireles and S. E. Ulloa, "Acceptor binding energies in GaN and AlN," [Physical Review B 58 3879 \(1998\)](#).
- ²⁰ Y. C. Shen, G. O. Mueller, S. Watanabe, N. F. Gardner, A. Munkholm, and M. R. Krames, "Auger recombination in InGaN measured by photoluminescence," [Applied Physics Letters 91 \(14\) 141101 \(2007\)](#).

-
- ²¹ T. E. Beechem, A. E. McDonald, E. J. Fuller, A. A. Talin, C. M. Rost, J.-P. Maria, J. T. Gaskins, P. E. Hopkins, and A. A. Allerman, "Size dictated thermal conductivity of GaN," [Journal of Applied Physics 120 095104 \(2016\)](#).
- ²² P. P. Paskov, M. Slomski, J. H. Leach, J. F. Muth, and T. Paskova, "Effect of Si doping on the thermal conductivity of bulk GaN at elevated temperatures – theory and experiment," [AIP Advances 7 095302 \(2017\)](#).
- ²³ F. Nippert, S. Y. Karpov, G. Callsen, B. Galler, T. Kure, C. Nenstiel, M. R. Wagner, M. Straburg, H.-J. Lugauer, and A. Hoffmann, "Temperature-dependent recombination coefficients in InGaN light-emitting diodes: Hole localization, Auger processes, and the green gap," [Applied Physics Letters 109 161103 \(2016\)](#).
- ²⁴ Y.-C. Tsai, C. Bayram, and J. P. Leburton, "Effect of Auger Electron-Hole Asymmetry on the Efficiency Droop in InGaN Quantum Well Light-Emitting Diodes," [IEEE Journal of Quantum Electronics 58 1 1 \(2022\)](#).
- ²⁵ S. Li, J. Schormann, D. J. As, and K. Lischka, "Room temperature green light emission from nonpolar cubic InGaN/GaN multi-quantum-wells," [Applied Physics Letters 90 071903 \(2007\)](#).
- ²⁶ M. R. Krames, O. B. Shchekin, R. Mueller-Mach, G. O. Mueller, L. Zhou, G. Harbers, and M. G. Carford, "Status and Future of High-Power Light-Emitting Diodes for Solid-State Lighting," [Journal of Display Technology 3 \(2\) 160 \(2007\)](#).
- ²⁷ T. Margalith, O. Buchinsky, D. A. Cohen, A. C. Abare, M. Hansen, S. P. DenBaars, and L. A. Coldren, "Indium tin oxide contacts to gallium nitride optoelectronic devices," [Applied Physics Letters 74 \(26\) 3930 \(1999\)](#).
- ²⁸ C. Bayram, J. Kim, C.-W. Cheng, J. Ott, K. B. Reuter, S. W. Bedell, D. K. Sadana, H. Park, and C. Dimitrakopoulos, "Vertical thinking in blue light emitting diodes: GaN-on-graphene technology," [Oxide-based Materials and Devices VI 93641C \(2015\)](#).
- ²⁹ J. K. Sheu, Y. K. Su, G. C. Chi, P. L. Koh, M. J. Jou, C. M. Chang, C. C. Liu, and W. C. Hung, "High-transparency Ni/Au ohmic contact to p-type GaN," [Applied Physics Letters 74 \(16\), 2340 \(1999\)](#).